

2 π -PHOTOPRODUCTION FROM CLAS AND CB-ELSA – THE SEARCH FOR MISSING RESONANCES –

U. THOMA FOR THE CB-ELSA AND CLAS COLLABORATION

*Thomas Jefferson National Accelerator Facility,
12000 Jefferson Avenue, Newport News, VA 23606, USA
E-mail: uthoma@jlab.org*

2 π -photoproduction is one of the promising reactions to search for baryon resonances that have been predicted but have not yet been observed. The $\gamma p \rightarrow p\pi^0\pi^0$ (CB-ELSA) and the $\gamma p \rightarrow p\pi^+\pi^-$ (CLAS) data show interesting resonance structures. A partial wave analysis (PWA) has to be done to determine which baryon resonances contribute, what their quantum numbers and their relative couplings to the different accessible $p2\pi$ -channels and to the photon are. First preliminary PWA-results on the lowest energy $p\pi^0\pi^0$ data ($\sqrt{s} < 1.8$ GeV) look very promising. From an extension of this analysis to higher energies combining the $p\pi^0\pi^0$ and the $p\pi^+\pi^-$ -data, one can expect interesting results on resonances decaying into $\Delta\pi$, $N\rho$, $N(\pi\pi)_s$, $N^*\pi$, and $\Delta^*\pi$.

1. Introduction

Quantum chromodynamics is believed to be the correct theory of strong interactions. Using perturbative methods we have access to QCD in two energy regimes: at high momentum transfer, and at very low energies in the realm of chiral perturbation theory. At medium energies, where the strong coupling constant is large and perturbative methods fail, our present understanding is still very limited, even if recent results of lattice QCD indicate that this situation might change in the future¹. This is the energy regime of meson and baryon resonances, and one of the key issues is to identify the relevant degrees-of-freedom and the effective forces between them. To reach this aim, a good understanding of the experimental spectrum of meson and baryon resonances and their properties is needed. Their comparison with different models, which have been developed to describe hadron properties and are based on different assumptions concerning the forces and relevant degrees-of-freedom, might lead to a deeper understanding of this energy regime. Quark models are usually based on the assumption that the strong interaction generates a confinement potential which grows linearly with the

distance between the quarks. But confinement alone does not describe the strong interaction properly. A residual interaction is needed which is of different origin in different models (e.g.: one-gluon exchange, instanton-induced forces, Goldstone boson exchange)². These models are in general amazingly successful in describing the spectrum of existing states. However, there is an interesting controversy. Constituent quark models usually predict many more resonances than have been observed so far. Two very different explanations have been proposed to explain this observation:

1) The "missing" states do not exist. As proposed e.g. by Lichtenberg, the nucleon resonances could have a quark-diquark structure. This reduces the number of internal degrees-of-freedom, and therefore, the number of existing states³. Of course, one might also think of other hidden symmetries. At a first glance, this explanation seems to be rather exotic. QCD does not give us any reason to believe that the three quarks shouldn't play an equal role in the nucleon. In addition, there are no hints from higher energy experiments for such a quark-diquark picture. On the other hand it is interesting to notice that the Regge trajectories for mesons and baryons are parallel (Figure 1). The observed similar dependence of the mass squared

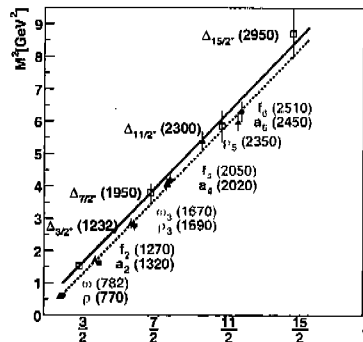


Figure 1. Regge trajectory for Δ -resonances with even orbital angular momentum L and $J=L+3/2$ in comparison to the meson trajectory ($J=L+S$), see also ⁴.

on the angular momentum seems to indicate that the acting force is very similar, too. This behavior could be easily understood in terms of a quark-diquark picture, with a diquark in a baryon replacing the antiquark in the meson. Most of the symmetric quark-model calculations fail to explain the N^* -Regge trajectories.

2.) The "missing" states have not been observed so far because of a lack of high quality data in channels different from πN . Most available experimental data stem from πN scattering experiments. If these states

decouple from πN they would not have been observed so far. This seems reasonable following quark model predictions^{5,6}.

Many of these unobserved states are expected to couple significantly to channels like $\Delta\pi$ or $N\rho$ and also to γp ^{6,7}. So photoproduction experiments investigating these channels have a great discovery potential if these resonances really exist. The investigation of 2π -photoproduction is not only interesting with respect to the search for the missing states, but it also allows to determine resonance properties like photocouplings and partial widths of known or less established resonances. This provides additional information which can be compared with different models and may therefore lead to a better understanding of the baryon resonances and strong QCD.

To investigate the $\Delta\pi$ and $N\rho$ -decay of baryon resonances, different isospin channels can be studied; two of them, the $\gamma p \rightarrow p\pi^0\pi^0$ and the $\gamma p \rightarrow p\pi^+\pi^-$ channels, will be discussed here. The $\gamma p \rightarrow p\pi^0\pi^0$ -channel is the one best suited to investigate the $\Delta\pi$ decay of baryon resonances. Compared to other isospin-channels, many non-resonant-“background” amplitudes cannot occur in this channel, like e.g. diffractive ρ -production or the Δ -Kroll-Rudermann term. In addition, the number of possible Born terms and t-channel processes is strongly reduced, e.g. π -exchange is not possible. This leads to a high sensitivity of this channel to baryon resonances decaying into $\Delta\pi$.

On the other hand, $\gamma p \rightarrow p\pi^0\pi^0$ does not provide any information on the $N\rho$ decay mode of baryon resonances. The reaction $\gamma p \rightarrow p\pi^+\pi^-$ allows the investigation of both the $\Delta\pi$ and the $N\rho$ decay of baryon resonances. Its disadvantage is that many other “non-resonant”-processes contribute which make this channel particularly difficult to analyze. Important “background” amplitudes are: the diffractive ρ -production, which is important especially at higher energies, and the direct $\Delta^{++}\pi^-$ production (Kroll-Rudermann term), which is strong at low energies. In addition, various Born-terms and t-channel exchange processes contribute.

If one combines the two data sets into one analysis, one can profit from the higher sensitivity of the $p\pi^0\pi^0$ channel concerning resonances decaying into $\Delta\pi$ and investigate the $N\rho$ channel at the same time. All common amplitudes are related by isospin, and the information provided by the $p\pi^0\pi^0$ channel simplifies the analysis of the more complicated $\gamma p \rightarrow p\pi^+\pi^-$ channel due to additional constraints.

In the following, the $p\pi^0\pi^0$ data taken by the Crystal Barrel experiment at ELSA (Bonn) will be discussed together with the $p\pi^+\pi^-$ data from

CLAS at Jefferson Laboratory starting with a short description of the two complementary detector systems.

The CLAS-detector ⁸ is a magnetic toroidal multi-gap spectrometer. Its magnetic field is generated by six superconducting coils arranged around the beam line to produce a field which is primarily pointing in the ϕ -direction. The detection system consists of drift chambers to determine the tracks of charged particles, gas Cerenkov counters for electron identification, scintillation counters for measuring time-of-flight, and electromagnetic calorimeters in the forward direction to detect showering particles like electrons and photons. Because of its good momentum resolution and large solid angle coverage, CLAS is very well suited to measure charged multiparticle final states.

In contrast to CLAS which is very well suited to measure charged particles but covers only an restricted angular range for photons, the Crystal Barrel detector is very well suited to measure photons. Its electromagnetic calorimeter consists of 1380 CsI crystals which cover about 98% of the 4π solid angle. The calorimeter surrounds a scintillating fibre detector used to identify charged particles leaving the target. It consists of 3 layers of scintillating fibres and surrounds the liquid-hydrogen target in the center of the detector. Using this setup, data at three different beam energies $E_{e^-} = 1.4$, 2.6, and 3.2 GeV have been taken covering baryon resonance masses up to 2.5 GeV. Recently the setup has changed: the electromagnetic calorimeter has been opened up in the forward direction to $\pm 30^\circ$, and TAPS is used as the forward detector.

2. The data

2.1. The $\gamma p \rightarrow p\pi^0\pi^0$ data from CB-ELSA ($E_{e^-} = 3.2$ GeV)

Figure 2 shows the evidence for $p\pi^0\pi^0$ and the $p\pi^0\eta$ final state in the $p4\gamma$ event sample. Both final states are clearly observed. The $p\pi^0\pi^0$ invariant mass (\sqrt{s}) shows two peaks: one around 1700 MeV which might be produced by N^* or/and Δ^* resonances and a second peak which is presumably due to the $D_{13}(1520)$. The lower edge in the spectrum is produced by the low-energy end of the tagging system. The complete lower mass peak is observed in the data which was taken with an electron beam of 1.4 GeV (Figure 6). Figure 2 also shows the $p\pi^0$ invariant mass for different bins in \sqrt{s} . These plots indicate how possible resonances in the corresponding mass ranges might decay. The lowest \sqrt{s} -bin is clearly dominated by $\Delta\pi$ -events. In the higher \sqrt{s} -bins, additional contributions become visible, like e.g. a

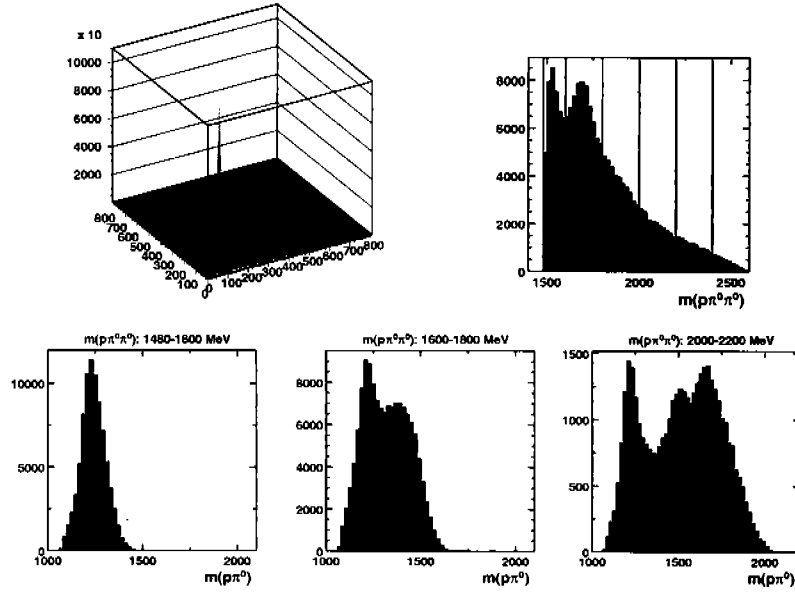


Figure 2. $p4\gamma$ events. Upper row: Left: $\gamma\gamma$ -invariant mass of one two-photon pair versus the $\gamma\gamma$ -invariant mass of the other two-photon pair. A clear peak due to $p\pi^0\pi^0$ events and smaller enhancements due to $p\pi^0\eta$ events are observed. Right: $p\pi^0\pi^0$ invariant mass (\sqrt{s}). Lower row: $p\pi^0$ invariant mass for different bins in \sqrt{s} , as mentioned on top of the plots. The plots are not corrected for acceptance, and no flux normalization was done (preliminary).

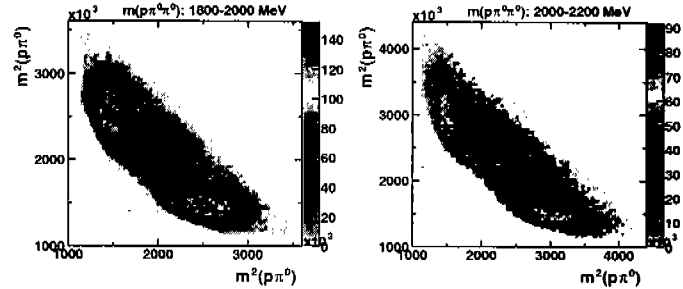


Figure 3. Dalitz plots for different \sqrt{s} -bins as given above the picture. The plots are not corrected for acceptance and no flux normalization was done (preliminary).

peak in the region of 1520 MeV and 1660 MeV. The latter is not due to a fall-off in phase space or acceptance. These structures are also visible in the corresponding Dalitz plots (Figure 3). Both plots show evidence for the $\Delta(1232)$ and for a vertical and horizontal band around $m_{p\pi^0}=1520$ MeV. In the plot of higher \sqrt{s} , additional indications for a band-like structure

around $m_{p\pi^0}=1660$ MeV are visible. The observed structures might hint at baryon resonances decaying into $\Delta(1232)\pi$, $X(\sim 1520)\pi$, and $X(\sim 1660)\pi$. To decide if the observed structures are really due to baryon resonances decaying into other baryon resonances and which quantum numbers contribute, a PWA has to be done. A first step in this direction, namely the preliminary results of a PWA of the lower energy $\gamma p \rightarrow p\pi^0\pi^0$ data ($E_e=1.4$ GeV), is discussed in section 3.

2.2. The $\gamma p \rightarrow p\pi^+\pi^-$ data from CLAS ($E_e=2.445$ GeV)

The CLAS data in terms of Dalitz plots for different regions in \sqrt{s} is shown in Figure 4. The lowest \sqrt{s} bin is clearly dominated by the Δ^{++} . At low energies the Δ -Kroll-Rudermann term dominates. With increasing \sqrt{s} the Δ^0 is more clearly visible and above the ρ -threshold the ρ starts to contribute and becomes rather prominent for higher \sqrt{s} . The ρ is clearly visible in the diagonal of the Dalitz plot for $\sqrt{s}=2.0$ -2.2 GeV, as well as in the corresponding $\pi^+\pi^-$ invariant mass. Whether part of the strong ρ -contribution is produced by baryon resonances decaying into $N\rho$ is again a question which can only be answered by a PWA.

Figure 5 shows the $p\pi^-$ invariant mass of the CLAS data together with

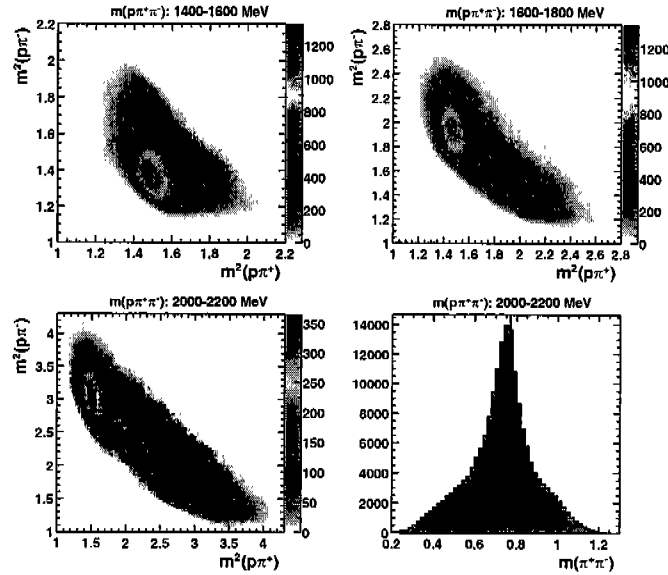


Figure 4. $\gamma p \rightarrow p\pi^+\pi^-$ data: The different plots show the data for different ranges in \sqrt{s} , as mentioned above the pictures. The plots are not corrected for acceptance and no flux normalization was done (preliminary).

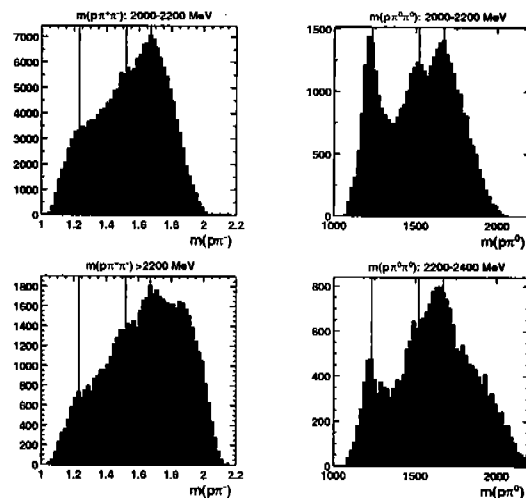


Figure 5. Left: $p\pi^-$ invariant mass of the CLAS data, right: $p\pi^0$ invariant mass of the CB-ELSA data. The different rows show the data for different ranges in \sqrt{s} , as mentioned above the pictures. The lines in the $p\pi^-$ invariant mass indicate the region of possible resonance contributions in the decay. The plots are not corrected for acceptance and no flux normalization was performed (preliminary).

the $p\pi^0$ invariant mass of the CB-ELSA data in order to investigate whether the same $p\pi$ -resonance structures occur. A close comparison of the two data sets shows that this is indeed the case. As expected, resonances are less pronounced in the CLAS data due to additional processes contributing to $\gamma p \rightarrow p\pi^+\pi^-$.

To decide finally if any of these interesting resonance structures are produced by decaying baryon resonances and to determine their quantum numbers, a PWA has to be done. A first step in this direction, namely a preliminary partial wave analysis of the lowest energy $\gamma p \rightarrow p\pi^0\pi^0$ data, will be discussed in the following section.

3. Preliminary partial wave analysis of the lowest energy $p\pi^0\pi^0$ -CB-ELSA data ($E_e = 1.4$ GeV)

The partial wave analysis of $\gamma p \rightarrow p\pi^0\pi^0$ discussed here presently takes only s-channel processes into account. An approximation which might be well justified for the $p\pi^0\pi^0$ data set but, of course, it has to be tested. In case of the more complicated $\gamma p \rightarrow p\pi^+\pi^-$ channel, non-s-channel processes such as t-channel exchange are known to contribute.

The $\gamma p \rightarrow p\pi^0\pi^0$ ($E_e = 1.4$ GeV) data was analyzed within the isobar

model using a Breit-Wigner description for the contributing resonances. An unbinned maximum-likelihood fit was performed. This fit method has the advantage of being event-based; it takes all the correlations between the five independent variables into account correctly. Therefore, all available information contained in an event is used. This is not the case when only differential cross sections are fitted. They represent one-dimensional projections of a five-dimensional space and, therefore, the information on the correlations is lost. In the past the latter method was usually used in baryon-resonance analyses.

To fit the $p\pi^0\pi^0$ data, resonances with different quantum numbers were introduced in various combinations allowing for the following decay modes: $\Delta(1232)\pi$, $N(\pi\pi)_s$, and $P_{11}(1440)\pi$. For a good description of the data the $P_{11}(1440)$, the $D_{13}(1520)$, and a $J^P = 3/2^-$ contribution in the mass region of 1700 MeV were needed. The latter might be due to the $D_{13}(1700)$ and/or $D_{33}(1700)$. In addition, the $P_{13}(1720)$ and the $F_{15}(1680)$ or the $P_{11}(1710)$ were necessary. Fits with the $F_{15}(1680)$ or the $P_{11}(1710)$ lead to a comparable description of the data. The masses and widths of the contributing resonances, along with their couplings and the phases between the different interfering amplitudes, were treated as free parameters. The masses and widths found for the resonances discussed above are in agreement with the values given by the PDG. The quality of the data description is shown in Figure 6 and Figure 7. Apart from some smaller deviations the data are well described. First combined fits with the $p\pi^+\pi^-$ -data indicate that the ambiguities discussed might be resolved in the coupled PWA of both data sets. Due to the additional information provided by the $p\pi^+\pi^-$ -data set, the isospin of the $3/2^-(1700)$ -contribution might be determined, and the $F_{15}(1680)/P_{11}(1710)$ -ambiguity might be resolved.

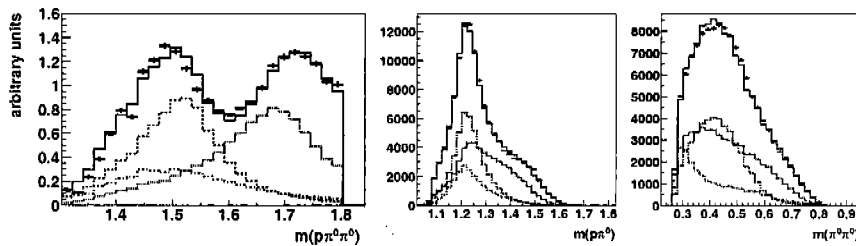


Figure 6. Left: $p\pi^0\pi^0$ -invariant mass: result of the PWA (solid curve) in comparison with the data (points with error bars). The data and the result of the PWA are divided by the distribution of the reconstructed Monte Carlo events. Center: $p\pi^0$ -invariant mass, right: $\pi^0\pi^0$ -invariant mass. Each plot shows the result of the PWA (solid curve), the contribution of the $D_{13}(1520)$ (dashed), the $P_{11}(1440)$ (dot-dashed), and the $J^P = 3/2^-(1700)$ (dotted).

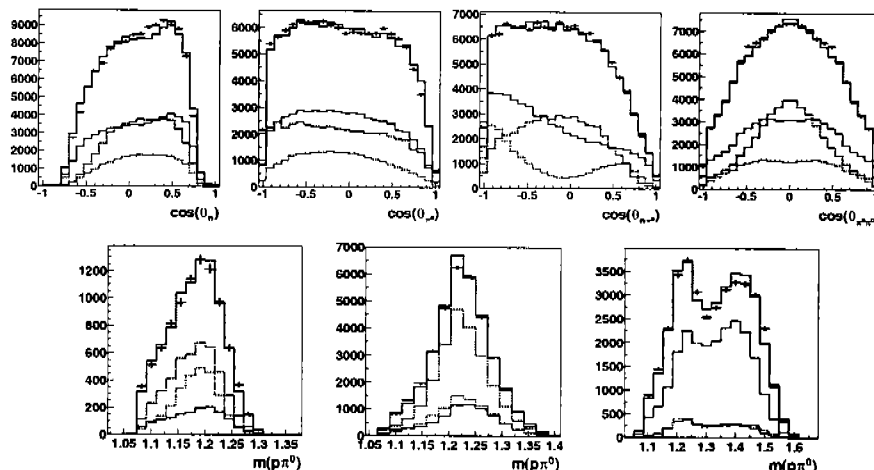


Figure 7. Upper row: Various angular distributions, lower row: $p\pi^0$ -invariant mass for different bins in \sqrt{s} , left: $\sqrt{s} = 1400 \pm 50$ MeV, middle: $\sqrt{s} = 1500 \pm 50$ MeV, right: $\sqrt{s} = 1700 \pm 50$ MeV. See Figure 6 for the meaning of the different curves.

Fig 8 shows the result of the PWA of the $p\pi^0\pi^0$ -data integrated over phase space. The resulting cross section is in good agreement with the results from TAPS⁹ and GRAAL¹⁰. One of the dominant contributions in this data set is the $D_{13}(1520)$ (see Figure 6). As an example for a result of the PWA, its properties as determined from the fits will be discussed qualitatively (further studies are necessary before the quantitative results can be given). The mass and width of the $D_{13}(1520)$ found in the PWA are in agreement with the PDG, $A_{3/2}$ was found to dominate $A_{1/2}$, and within the $p\pi^0\pi^0$ final state the $\Delta\pi$ decay mode is dominant (see also Figure 7). In addition, it was found that the decay into a $\Delta\pi$ S-wave is stronger than the corresponding decay into a $\Delta\pi$ D-wave. The latter result is in agreement with the results of a recent multi-channel analysis¹¹.

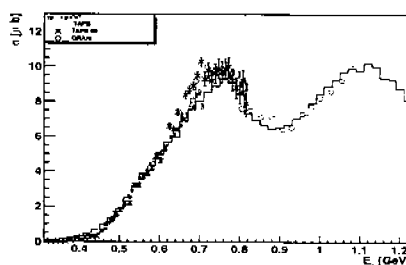


Figure 8. The $\gamma p \rightarrow p\pi^0\pi^0$ cross section as determined from the PWA (solid curve) in comparison with GRAAL (circles) and TAPS (crosses).

4. Summary

Preliminary results of the event-based PWA of the $\gamma p \rightarrow p\pi^0\pi^0$ data set look very promising. The description of the data achieved using only s-channel amplitudes is quite good, and the parameters of well known resonances are well reproduced. Of course, the influence of non-s-channel amplitudes on the results has to be tested.

The higher energy $p\pi^0\pi^0$ (3.2 GeV) and the $p\pi^+\pi^-$ data show very interesting resonance structures. These data sets cover the mass region where many of the so far non-observed baryon resonances should exist. An extension of the PWA to include these data sets is in progress, and the first combined fits of the $p\pi^0\pi^0$ and the $p\pi^+\pi^-$ data set have been performed.

This PWA should help us to answer the question which baryon resonances exist and couple to γp and to at least one of the different $p2\pi$ -channels. Of course, this analysis will also allow us to determine the relative couplings of the contributing resonances to the different $p2\pi$ decay channels like $\Delta\pi$, $N\rho$, $N(\pi\pi)_s$, $N^*\pi$, and $\Delta^*\pi$.

Acknowledgments

The author acknowledges an Emmy Noether grant from the Deutsche Forschungsgemeinschaft. The Southeastern Universities Research Association (SURA) operates the Thomas Jefferson National Accelerator Facility for the United States Department of Energy under contract DE-AC05-84ER40150.

References

1. F. X. Lee this conference.
2. B Metsch, W. Plessas, S. Capstick this conference.
3. D. B. Lichtenberg, Phys. Rev. **178**, 2197 (1969).
4. E. Klempt, Phys. Rev. **C66**, 058201 (2002).
5. S. Capstick and W. Roberts, Phys. Rev. **D47**, 1994 (1993).
6. S. Capstick and W. Roberts, Phys. Rev. **D49**, 4570 (1994).
7. S. Capstick, Phys. Rev. **D46**, 2864 (1992).
8. B. Mecking *et al.*, accepted by NIM, *The CEBAF Large Acceptance Spectrometer*.
9. M. Wolf *et al.*, Eur. Phys. J. A9, 5 (2000), M. Kotulla, Dissertation Universität Giessen, Dez. 2001.
10. Y. Assafiri *et al.*, AIP Conference Proceedings 610, INPC 2001, 362.
11. T. P. Vrana *et al.*, Phys. Rept. 328, 181 (2000).